Spectrochimica Acta Part A: Molecular and Biomolecular Spectroscopy 329 (2025) 125648

Contents lists available at ScienceDirect

Spectrochimica Acta Part A:
Molecular and Biomolecular Spectroscopy

journal homepage: www.journals.elsevier.com/spectrochimica-acta-part-a-molecular-and-biomolecular-spectroscopy

Raman scattering of water in vicinity of polar complexes: Computational insight into baseline subtraction

Christina Karafyllia [a,b], Jiří Kessler [b], Jana Hudecová [c], Josef Kapitán [c], Petr Bouř [b,d,*]

[a] Faculty of Sciences, Aristotle University of Thessaloniki, University Campus 54124, Thessaloniki, Greece
[b] Institute of Organic Chemistry and Biochemistry, Academy of Sciences, Flemingovo náměstí 2, 16610, Prague, Czech Republic
[c] Department of Optics, Palacký University, 17. listopadu 12, Olomouc 771 46, Czech Republic
[d] Department of Analytical Chemistry, University of Chemistry and Technology, Technická 5, 16628 Prague, Czech Republic

HIGHLIGHTS

- Non-additive effects often prevent baseline subtraction in Raman spectra.
- Anions affect Raman scattering of water more than cations.
- Molecules in resonance increase the signal of water.
- Cluster-based molecular modeling reveals the underlying mechanisms.

GRAPHICAL ABSTRACT

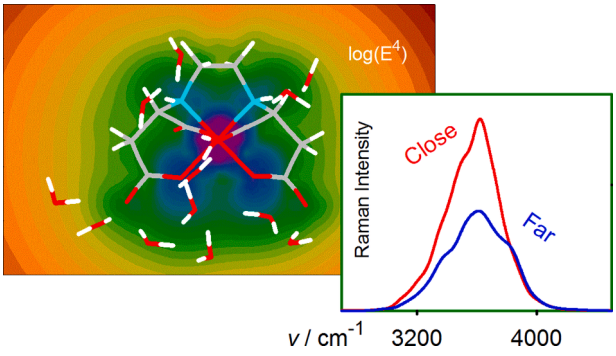

ARTICLE INFO

Keywords:
Raman scattering
Resonance effects
Density functional theory
Baseline subtraction
Molecular modeling
Ionic solutions

ABSTRACT

Water is a greatly convenient solvent in Raman spectroscopy. However, non-additive effects sometimes make its signal difficult to subtract. To understand these effects, spectra for clusters of model ions, including transition metal complexes and water molecules, were simulated and analyzed. A combined molecular mechanics/quantum mechanics approach was taken to reveal how relative Raman scattering intensities depend on the distance from the solute and the excitation wavelength. The computations indicate a big effect of solute charge; for example, the sodium cation affects Raman scattering by water to a lesser extent than the chlorine anion. The modeling was able to qualitatively reproduce the experimental observation that a solution of a simple salt may work as a baseline better than pure water in many Raman experiments. For absorbing species, an additional scattering boost occurs due to the resonance effect. Simulations thus provide useful insight into solute–solvent interactions and their effects on measured spectra.

* Corresponding author at: Institute of Organic Chemistry and Biochemistry, Academy of Sciences, Flemingovo náměstí 2, 16610, Prague, Czech Republic.
E-mail address: bour@uochb.cas.cz (P. Bouř).

https://doi.org/10.1016/j.saa.2024.125648
Received 18 November 2024; Received in revised form 18 December 2024; Accepted 19 December 2024
Available online 20 December 2024

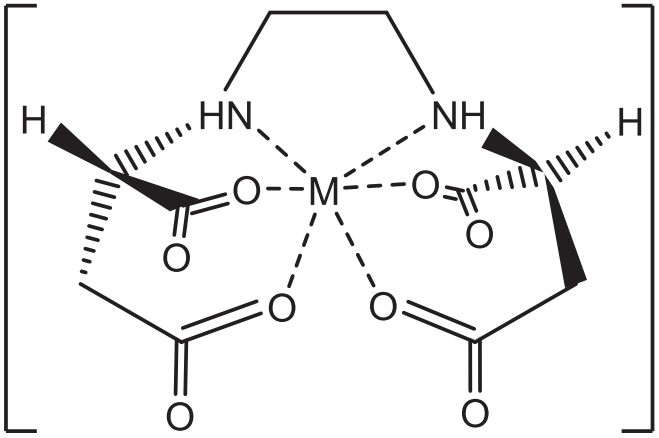

Fig. 1. Structure of (*S*,*S*)-N,N-ethylenediaminedisuccinic (EDDS) acid complexes (e.g., M = Co^{III}, Al^{III}, Mg^{II}).

1. Introduction

It is well known that Raman scattering by water sensitively reflects not only its temperature, but also the compounds dissolved in it. For ions, this can be related to the structure of the solvation shell [1,2]. However, the dependence is quite complex. For example, whereas Na_2SO_4 solutions produce a specific OH stretching signal, the spectrum of Na_3PO_4 is close to that of pure water, and D_2O in H_2O causes similar changes as some monovalent ions. Some metal ions provide characteristically shaped OH stretching bands [3]. With the aid of *ab initio* molecular dynamics, one can potentially decompose overall spectra into contributions from individual species in the solution [4]. For elements forming strong coordination bonds to water, such as magnesium or transition metals, new bands can be observed in the spectra [5,6].

The sensitivity of Raman scattering by water to the dissolved species brings about practical problems for baseline subtraction that make it difficult to subtract the water signal from that of the solute under investigation. The topic of baseline subtraction is discussed in detail, for example, in ref. [7]. In the present study, we focus on gaining a deeper insight, trying to understand how Raman scattering by water is modified and to what distance from the solute and attempting to ascertain whether the excitation wavelength is important.

The immediate motivation behind this study stemmed from previous investigations of EDDS complexes (Fig. 1), where direct subtraction of the water background proved problematic [8]. For example, the CoEDDS complex was strongly absorbing since the S_3 electronic transition was in resonance [9] with the 532 nm laser radiation, and an unusually strong residual water signal remained after the subtraction. In addition, under the conditions of the resonance experiment (a rotating cell, strong absorption, unknown temperature), the background subtraction could not be done reliably. But also for non-resonating EDDS complexes, such as with aluminum or magnesium, and the residual water signal although smaller was still there. In addition, in these cases, some subtraction algorithms even produced unphysical negative Raman intensities.

As demonstrated below, modeling based on molecular dynamics–density functional theory at least partially explains these observations. For example, the computations clearly show that water molecules that are close to the solute may exhibit enhanced scattering in both resonance and far-from-resonance Raman spectroscopy. The models also confirm the dominant effect of solute negative charges and polar molecular parts on the shape of spectra. This can be confirmed by experiment when the Cl^- ion produces similar effect as the $EDDS^-$ anion. We thus believe that these simulations provide insight that is generally useful in practical Raman spectroscopy.

2. Methods

The preparation of the complexes and spectra measurement are described in ref. [8]. Briefly, a Zebr Raman optical activity spectrometer was used, operating with 532 nm excitation. The CoEDDS complex was prepared by chemical synthesis, while the other ones were prepared by mixing EDDS and chloride ($AlCl_3$, $MgCl_2$) solutions and adjusting pH by NaOH to about 7.5. Final concentrations used for the measurements were 0.012 M for CoEDDS and 0.33 M for AlEDDS and MgEDDS.

To understand the effect of the complexes on Raman scattering of the water solvent, sodium and chlorine ions, CoEDDS and AlEDDS complexes, and water-in-water clusters were used as the model systems. Cobalt and aluminum complexes were selected because they allowed us to compare the results of resonance and non-resonance Raman spectroscopy, respectively. An ensemble of geometries was obtained by employing molecular dynamics (MD) simulations. The solutes were placed into a cubic 40^3 $Å^3$ box otherwise filled with water, and MD simulations were run within the Amber [10] software environment. An *nVT* thermodynamic ensemble was simulated using the Amber force field [11] (TIP3P [12] for water), a 1 fs integration step, and temperature stabilization at 300 K. The complex geometries were constrained

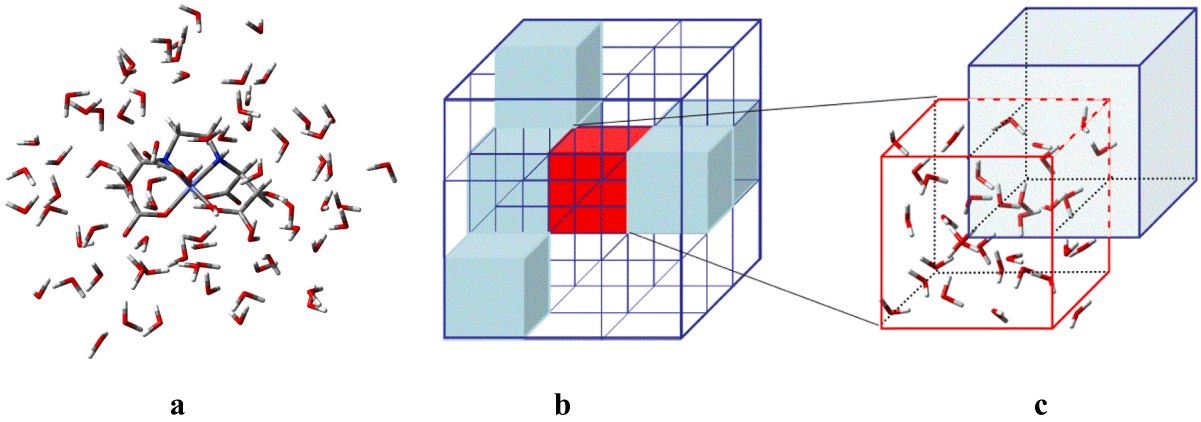

Fig. 2. (a) Example MD geometry of CoEDDS in cluster with 72 water molecules, (b) crystal-like water model where for an arbitrary "3×3×3" box (b) the force field was calculated from smaller fragments consisting of periodic MD boxes and shifted partially overlapping ones (c). The shifted boxes were placed at the sides, edges and corners of the small box, so, for example, all molecules in the central red box could fully interact with the closest environment. Then, the dynamic matrix (force field) and Raman spectrum were calculated (cf. also ref. [16]). (For interpretation of the references to colour in this figure legend, the reader is referred to the web version of this article.)

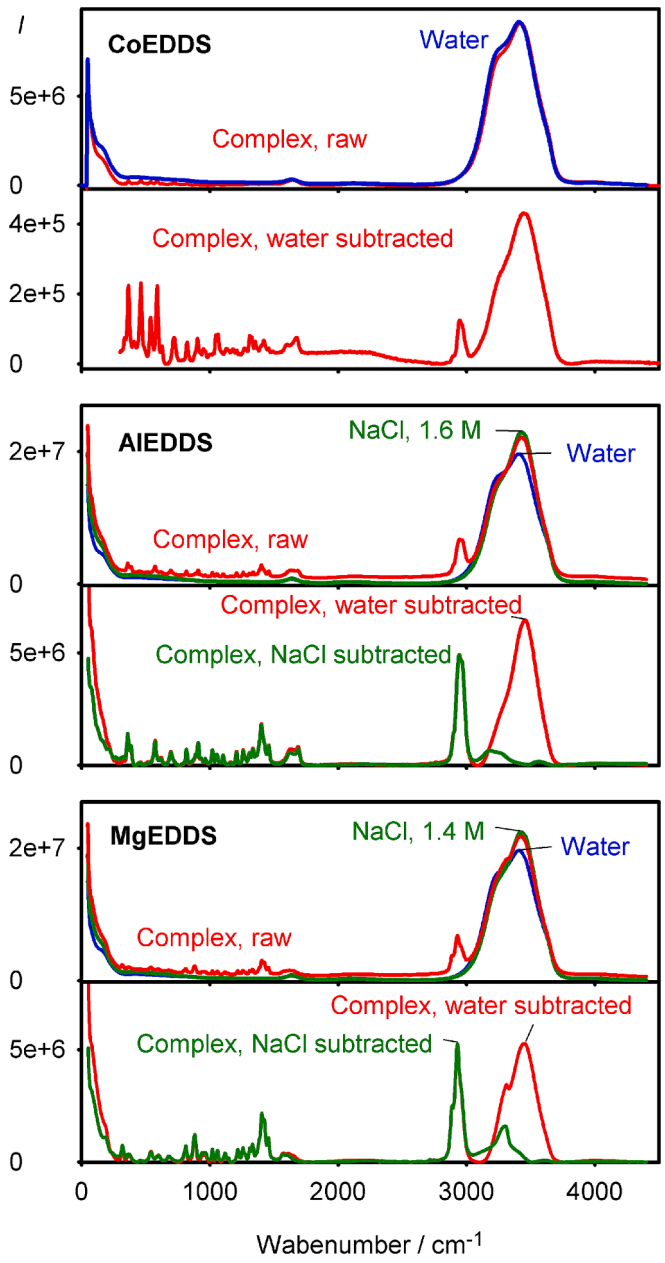

Fig. 3. Experimental Raman spectra of water, NaCl solution, and the CoEDDS, AlEDDS, and MgEDDS complexes before and after the background subtraction.

to those optimized at the B3LYP [13]/6–311++G**/PCM [14] (H_2O) level. After equilibration, 20 snapshot geometries were selected at 1 ps intervals, and water molecules further than ~ 5 Å from the solute were deleted.

The geometries of the resulting clusters (e.g. in Fig. 2**a**) were partially optimized by energy minimization using normal-mode coordinates [15]. This ensures that the MD geometry is largely conserved whereas coordinates important for the vibrations of interest are relaxed. Vibrational frequencies and Raman intensities were calculated at the harmonic level. Computations of the gradient for optimization and spectral calculations were performed at the B3LYP/6-31G**/PCM(H_2O) level, using the software Gaussian (Rev. C01, https://www.gaussian.com). For trial computations, the 6–311++G** basis set was used, which provided similar results as 6-31G**, i.e., frequencies within ~ 1 % and lower absolute (by ~ 20 %) but similar relative intensities. For the large clusters, the bigger basis set, however, did not enable extensive averaging of the geometries. The outputs were analyzed using scripts developed by us. The approximate contributions of individual water molecules to Raman scattering were estimated by erasing all polarizability derivatives not related to the three water atoms. Calculated Raman intensities are given in arbitrary units; smooth spectra were obtained by convolution with a Gaussian function.

An alternate, crystal-like model of water [16] was also tried, where a smaller 10^3 Å^3 water box was subjected to MD, producing snapshot geometries. For each snapshot, in a 3×3×3 superbox (Fig. 2**b**) the force field was created based on smaller fragments (Fig. 2**c**). The geometries of the smaller overlapping clusters were partially optimized using the normal-mode coordinates, and force field and polarizability derivatives were calculated, all at the B3LYP/6-31G**/PCM(H_2O) level. The vibrational parameters were transferred back onto the superbox, using Cartesian coordinate-based tensor transfer (CCT) [17,18]. Finally, a dynamic matrix and zero phonon modes [19] were calculated, and Raman spectra for 20 snapshots were averaged.

Simpler models consisted of one water molecule in the vicinity of various ions, for which Raman intensities were calculated with the B3LYP functional, using Gaussian. In this case, the larger 6–311++G** basis set could be used. In addition, following the perturbation scattering theory, according to which signal enhancement in vicinity of a polarizable particle is proportional to E^4/E_0^4 (E being the actual and E_0 the laser electric intensity; in the computation it is convenient to set E_0 equal to 1) [20,21]. For a selected MD snapshot, we calculated an enhancement map in the vicinity of the CoEDDS complex, using the dynamic electron density obtained at the B3LYP/6–311++G** level and the procedure described in ref. [20].

3. Results and discussion

3.1. Water subtraction in experimental spectra

In Fig. 3 we can see that the water background cannot be completely subtracted for the resonating CoEDDS complex, in particular within the OH stretching region (~3100–3700 cm^{-1}). The intensity of the residual band at 3514 cm^{-1} is about three times bigger than that of the CH stretching of EDDS (at 2945 cm^{-1}), for example. Although the residual band can still contain a small contribution from EDDS N-H stretching and the intensity is somewhat dependent on the subtraction algorithm, the result indicates that the complex significantly enhances Raman scattering of the solvent, most probably in its vicinity.

For MgEDDS and AlEDDS the residual ~ 3453 cm^{-1} bands are smaller than for CoEDDS, their intensities are comparable with the CH stretching band at 2929 cm^{-1}. Interestingly, using spectra of NaCl solutions instead of distilled water as a background provided much better results, where the water OH stretching signal is almost eliminated and a ~ 3300 cm^{-1} band of NH stretching is visible only in this region.

3.2. Dependence of the signal of one water molecule on its environment

First, we ran simpler computations to get a feeling of the effects of ions in the vicinity of Raman-scattering water molecules. For Na^+ and Cl^- ions, examples of integral intensities integrated over OH bending and symmetric and asymmetric OH stretching (δ, *vs*, *vA*) bands are presented in Fig. 4. We can see that the effect of Na^+ and Cl^- ions very much depends on the geometry and that only limited conclusions can be drawn about the behavior of bulk water. Nevertheless, some interesting trends can be traced out: (1) the OH bending signal always increases in the vicinity of Cl^- whereas it decreases around Na^+, (2) OH stretching behaves in a more complex way, (3) OH stretching intensity is influenced by the presence of ions at larger distances (~ 10 Å) than OH bending is (~ 7 Å), (4) chlorine generally elicits bigger effects than sodium.

For another simple system composed of one water molecule in the vicinity of a CoEDDS complex (Fig. 5), we explored the dependence of the OH scattering intensity on the excitation wavelength. When

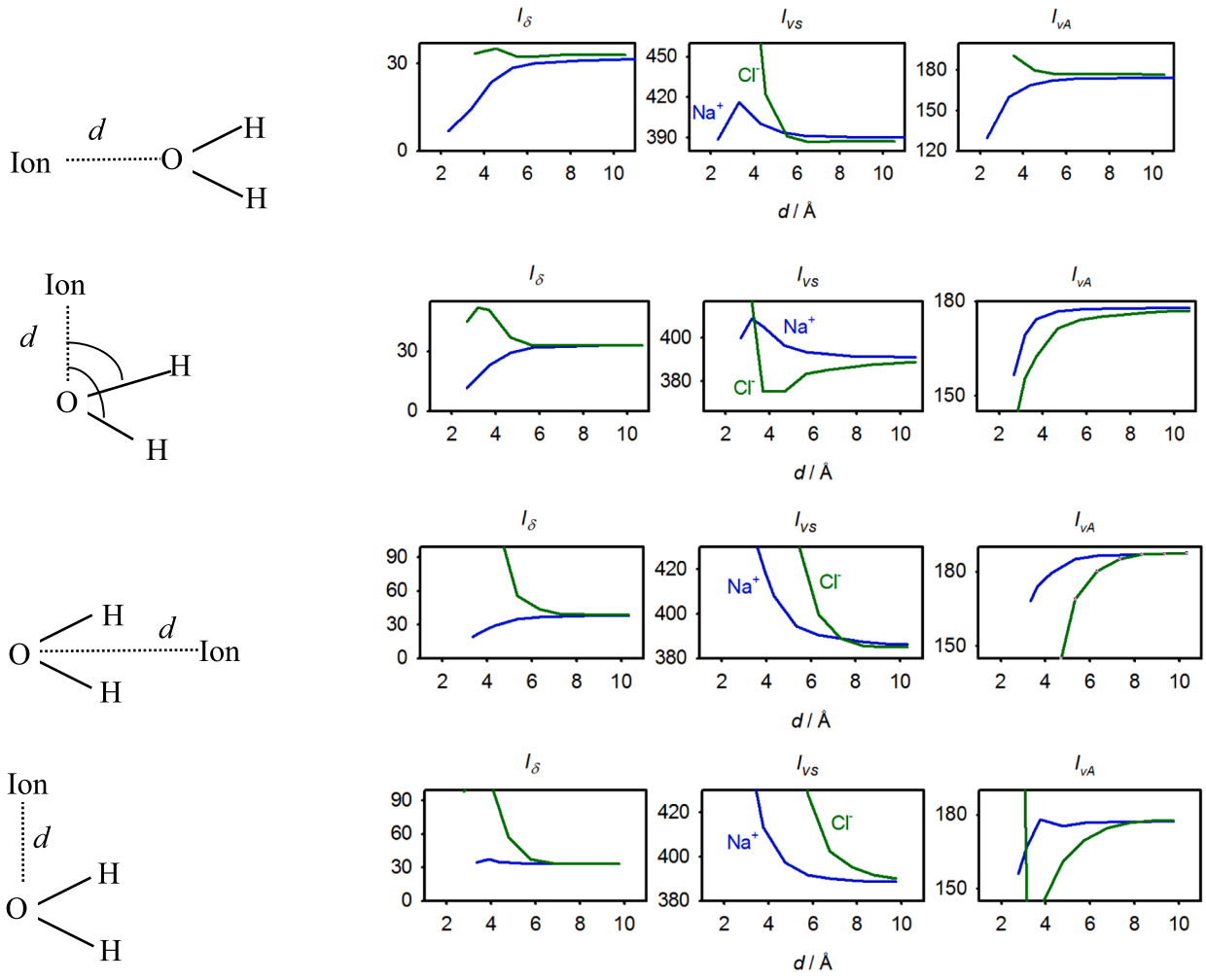

Fig. 4. Integral intensities [integrated over HOH bending, δ, and symmetric (*vs*) and asymmetric (*va*) OH stretching bands] of the signal of water molecules in vicinity of Na^+ and Cl^- ions as obtained at the B3LYP/6–311++G** level.

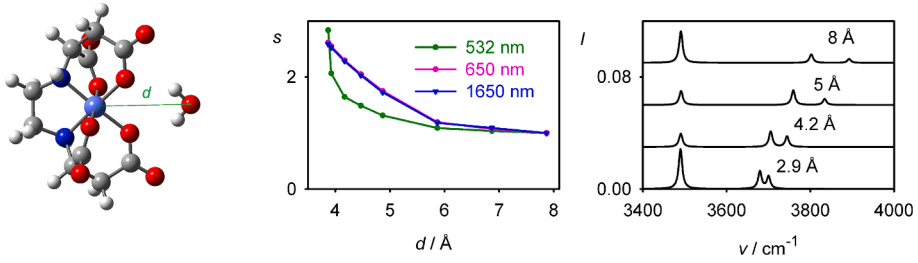

Fig. 5. Symmetric complex of CoEDDS and water, the dependence of water OH stretching integral intensity (*s*) on distance (in Å), and the dependence of the spectra for 532 nm excitation.

normalized to the largest distance of 8 Å, in the far-from-resonance (FFR) cases (650 and 1650 nm) the intensity increases about 2.6-fold at the equilibrium distance of 3.9 Å. This happens also with 532 nm excitation, close to the $S_0 \rightarrow S_3$ absorption band of the CoEDDS complex [8], but significant increases happen at shorter distances than in the FFR case. It should be noted that absolute intensities (which are normally not measured) are very different for the three excitation levels, being approximately inversely proportional to the fourth power of the wavelength ($\sim \lambda^{-4}$) [9,22]. However, this does not affect the relative band ratios, and this factor is omitted from the simulations. We can see that, besides the integral intensities, the band positions and relative intensities also change in the vicinity of the complex. The wavenumber (position) changes may be related to the formation of hydrogen bonds with the complex, which requires electron transfer from OH covalent bonds of water, making them weaker.

3.3. Bulk models – Resonance versus far from resonance

Some of the trends observed in the results for the separate water molecules shown above can also be seen in the bulk models. For AlEDDS, integral intensities of individual water molecules are plotted in Fig. 6**a** as dependent on their closest distance to an EDDS oxygen atom. Both the OH bending and the OH stretching intensities increase in the closest vicinity of the solute, but this intensity boost is quickly lost at greater

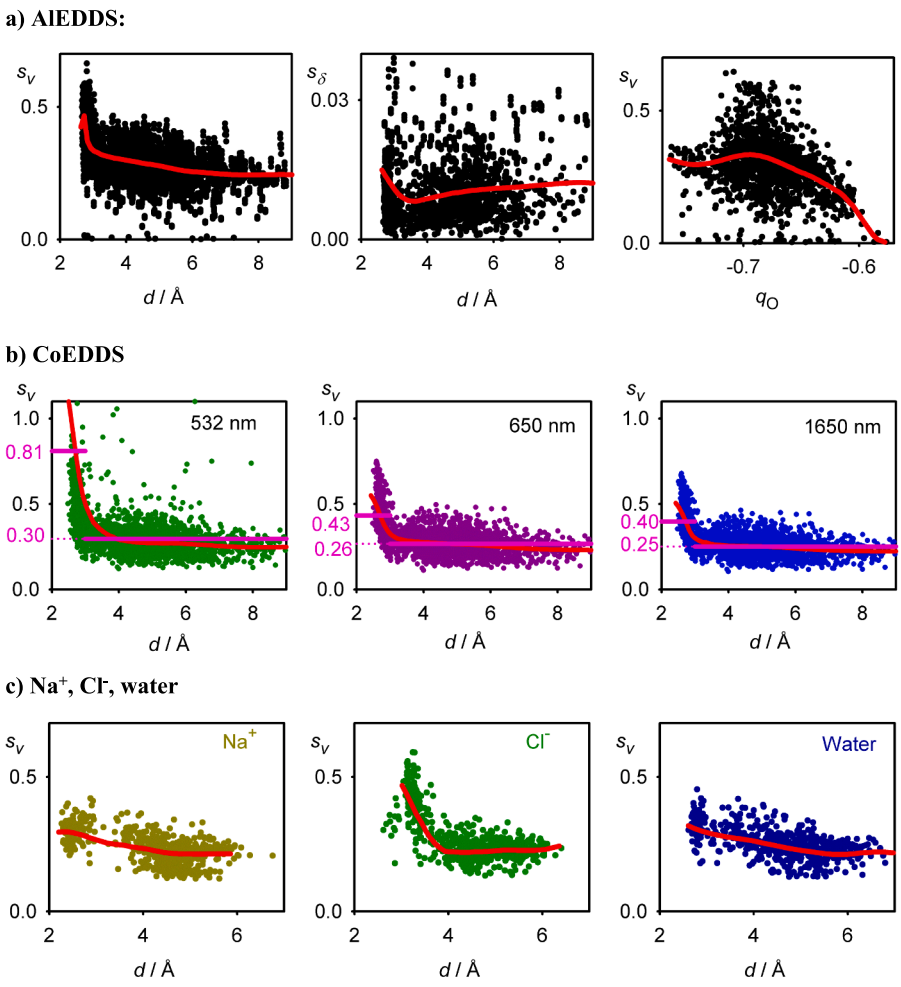

Fig. 6. (a) AlEDDS-water clusters, dependence of integral Raman intensities (s_ν OH stretching, s_δ bending) of individual water molecules on their distance from the closest oxygen atom of EDDS (d), and dependence of s_ν on the Mulliken charge of the oxygen atom of water (q_O). (b) CoEDDS–water clusters, dependence of s_ν on d for three excitation wavelengths. The magenta lines and numbers indicate plain averages within 0–3 Å and 3–9 Å. (c) Dependencies of $s_\nu(d)$ on the distance for sodium, chlorine and water clusters. In all graphs, the red curves indicate approximate floating averages. (For interpretation of the references to colour in this figure legend, the reader is referred to the web version of this article.)

distances. The OH stretching vibrations seem to be more sensitive than OH bending, which can also be interpreted as the OH bending intensities being more dependent on adjacent hydrogen network. Indeed, in relative terms, its intensity varies much more. Occasionally, near-zero intensities were calculated when the calculated frequencies were outside the integration limits of 1400–1900 cm^{-1} for bending and 2500–4500 cm^{-1} for stretching. These are, however, quite rare and do not affect the overall trends. We also see a weak correlation between the intensities and the Mulliken charge on the oxygen atom of water (q_O). A more negative charge favors greater Raman scattering intensity, which is possibly related to the increased number of polarizable electrons.

Next, we focused on OH stretching bands, which appear to be more sensitive and also more important, from the experimental point of view, than OH bending. For the CoEDDS complex, which strongly absorbs visible light [8], the water OH integral intensities in relation to the water-to-EDDS oxygen distance are plotted for three excitation frequencies in Fig. 6**b**. As in the simpler model (Fig. 5), 532 nm excitation enhances relative Raman intensities of some water molecules. From the plain averages in Fig. 6**b** (indicated by the magenta numbers), we see that water molecules closer than 3 Å result in much greater average integral intensity for excitation at 532 nm (0.81) than for excitation at 650 and 1650 nm (0.43 and 0.40). For water molecules further from the complex (> 3 Å), however, the intensities are similar (0.3, 0.26 and 0.25). In other words, for absorbing compounds the modeling suggests

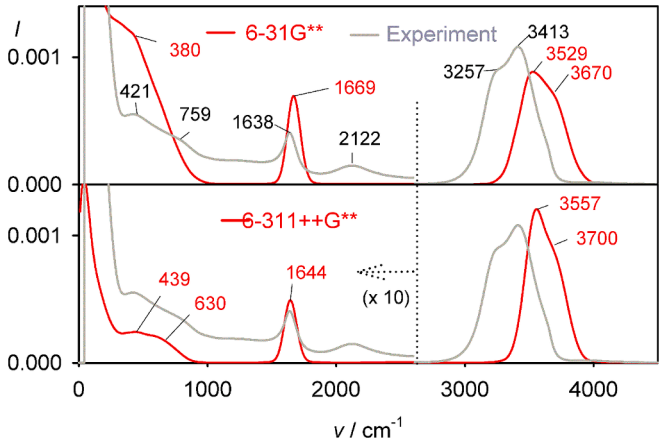

Fig. 7. Calculated (B3LYP, crystal-like model, smoothed average from 20 snapshots) and experimental spectra of pure water at 20 °C.

an additional intensity boost for close water molecules, at least partially explaining the experimental observation (Fig. 3, ref. [8]).

For the 532 nm excitation wavelength, integral intensities are plotted for clusters containing sodium and chlorine ions and for water

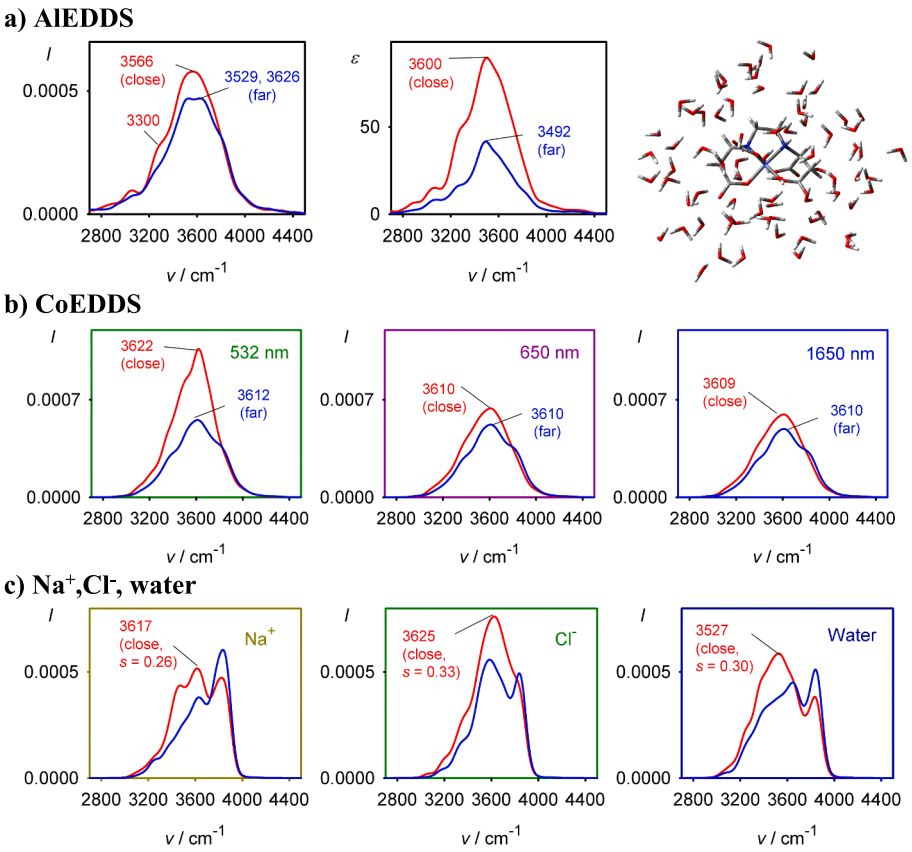

Fig. 8. (a) AlEDDS, calculated (B3LYP/6-31G**, smoothed average from 20 snapshots) Raman (*I*, for 532 nm excitation) and IR (ε) spectra from water molecules in AlEDDS–water clusters, for water molecules closer to (within the 0–5 Å range) and further away (4–6 Å) from oxygen atoms of EDDS, normalized to one water molecule; frequencies of maxima are indicated. (b) CoEDDS, analogous notation, Raman spectra for three excitation wavelengths. (c) Raman spectra (532 nm) calculated for Na^+, Cl^- and H_2O, using analogous notation; *s* denotes integral intensities.

clusters in the water-in-water model (Fig. 6**c**). For the latter, the dependence on distance is obviously an artifact: Water molecules far from the central molecule are in contact with the PCM dielectric environment, mimicking directional hydrogen binding only partially [23]. Having this in mind, it is remarkable that the Na^+ cation almost does not affect Raman scattering by water molecules in its vicinity whereas Cl^- does, and in a similar way as AlEDDS and CoEDDS anions do. This justifies using the NaCl instead of water as a baseline (Fig. 3).

3.4. Spectral shapes

For the crystal-like water model, Raman spectra obtained with the 6-31G** and 6–311++G** basis sets are compared with experimental spectra in Fig. 7. In Raman experiments, OH stretching generates a band at 3413 cm^{-1} with a shoulder at around 3257 cm^{-1}. By contrast, in the computations the lower-wavenumber band (3529 and 3557 cm^{-1} for 6-31G** and 6–311++G**) is stronger than the higher-wavenumber one (3670/3700 cm^{-1}). Because the ratio is dependent on anharmonic and temperature effects, and because it is generally difficult to obtain computationally, even with *ab initio* MD [24,25], we consider the agreement satisfactory for investigating changes in relative intensity caused by solutes. The calculated bandwidths seem reasonable as well. Although the wavenumber is about 250 cm^{-1} greater than in experimental spectra, this is a usual error given by the harmonic approximation and use of the double-hybrid functional [26,27], The combination 2122 cm^{-1} band in the experimental spectrum is not reproduced by the harmonic model. The wavenumber, bandwidth and relative intensity of the (experimentally ascertained) 1638 cm^{-1} bending vibration are predicted reasonably well. The two basis sets produce similar results with respect to the OH bending and stretching signals discussed in the present study; the bigger one seems to be much more appropriate for the lower-wavenumber (< 1000 cm^{-1}) region. However, this region is not in focus of the present study and we find the 6-31G** basis set acceptable as well, allowing us to compute larger solvent–solute clusters.

In Fig. 8, we focus on the OH stretching band and simulated Raman spectra for water molecules closer to and further away from the solute. For the AlEDDS complex [part (a) of the figure; IR spectra also included] intensity changes in the Raman spectra are smaller than in the IR spectra, but they are also quite pronounced. This is consistent with the previous observation (Figs. 5, 6) that mainly in the vicinity of the polar extremities of EDDS (i.e. carboxyl oxygens) the signal can be amplified. A detailed analysis of the IR pattern would be beyond the scope of the present article. In the Raman spectra, apart from the intensities, the band shape changes as well, as far water signals with maxima at 3529/3636 cm^{-1} approach those of the "pure water" model (cf. Fig. 7). Closer water molecules produce a maximum at 3566 cm^{-1} and a shoulder at 3300 cm^{-1}. Molecules further than 6 Å were excluded to avoid terminal effects.

Similar trends can be seen for the CoEDDS complex (Fig. 8**b**). However, since the excitation wavelength of 532 nm is close to the absorption band, the enhancement of Raman signals for water molecules close to the complex is much greater. This has been already seen in an alternate representation in Fig. 6. In addition, the bandshape changes more for 532 nm than for the other two excitation wavelengths, as water molecules close to the complex give a sharper maximum at 3622 cm^{-1}.

In the spectra simulated for Na^+, Cl^- and water (Fig. 8**c**), we may disregard the band around 3800 cm^{-1} (blue curves), as an artifact caused by water molecules close to the PCM environment. This band is absent in the crystal-like model (Fig. 7). Focusing on the water close to

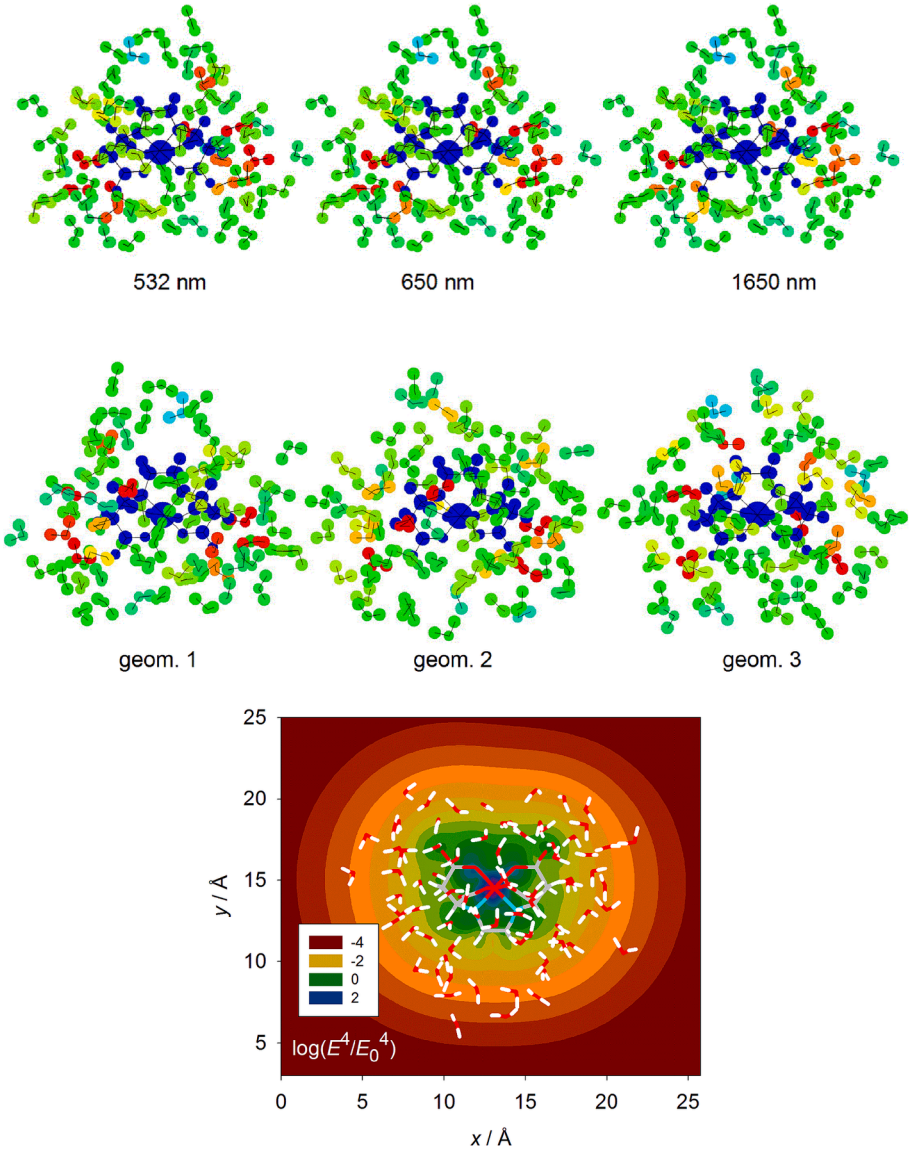

Fig. 9. CoEDDS–water clusters. *Top:* integral OH stretching intensities for individual water molecules, one MD snapshot, three excitation wavelengths. *Middle:* three geometries, 650 nm excitation; blue/green indicate the lowest intensities, and red indicates the highest intensities. *Bottom:* relative enhancement calculated from the dynamic electron density (logarithmic scale). (For interpretation of the references to colour in this figure legend, the reader is referred to the web version of this article.)

the solute (red curves in Fig. 8**c**), we see that Raman scattering by water molecules close to the sodium ion does not differ that much from that by H_2O molecules in pure water. The sodium gives smaller integral intensity (0.26 *vs* 0.30), consistently with the dependencies visible already in Fig. 6**c**. The band maximum shifts from 3527 to 3617 cm^{-1}. For the chlorine ion, the band shape changes more, with a downward shift of the maximum (to 3625 cm^{-1}) and an intensity increase to 0.33.

3.5. Qualitative visualization

Fig. 9 illustrates the complex relationship between the environment and Raman intensities of water molecules. The relative intensities are encoded in false colors, the computations are for the CoEDDS complex. For example, the excitation wavelength does not seem to have a significant effect on the relative intensities. By contrast, there is a systematic intensity increase in the vicinity of the most polar molecular parts – the carboxyl residues. This happens also with water molecules not directly hydrogen-bonded to EDDS, which suggests that the enhancement comes to a great extent from the EDDS electrostatic field. At the bottom of the figure, the enhancement estimated from the dynamic electric field at 532 nm is plotted. This indicates the short-range of the resonance enhancement and its dependence on the shape of molecules. However, the magnitude of the enhancement is strongly dependent on the bandwidth parameter chosen for the simulation (a value of 5 nm was used), and this dynamic field model also does not capture fine electronic effects such as occasional enhancement for water molecules further from the solute.

4. Conclusion

We have devised several computational models to improve our understanding of certain difficulties concerning the subtraction of the background water signal in Raman spectra of EDDS complexes. In particular, the results of our experiments suggest that compounds absorbing excitation light behave differently from transparent ones and that both types of compounds modify the Raman scattering by water in their vicinity. This is confirmed by the modeling, which provides additional findings, such as that the polar extremities (carbonyl oxygens) of

transition metal complexes are the most influential in this respect.

Our simulations and experiments also give merit to the use of aqueous solutions of simple salts, such as NaCl, instead of pure water. If they have ionic strength similar to that of the solute being analyzed the background subtraction can be done much more efficiently. With transparent compounds, the solute affects the solvent scattering only up to relatively short distances (< 4 Å). By contrast, with absorbing compounds, the resonance effect reaches much further, although accurate experiments and modeling remain much more challenging in this case and further investigations are desirable in the future. In spite of the current limits, we believe that our computational approach might prove generally useful in many branches of Raman spectroscopy. Future, more precise simulations of the Raman signal of water molecules in different environments could make the technique suitable even for new analytical applications.

Declaration of competing interest

The authors declare that they have no known competing financial interests or personal relationships that could have appeared to influence the work reported in this paper.

Acknowledgment

The work was supported by the Grant Agency of the Czech Republic (22-04669S).

Data availability

Data will be made available on request.

References

[1] M. Ahmed, V. Namboodiri, A.K. Singh, J.A. Mondal, S.K. Sarkar, How ions affect the structure of water: a combined raman spectroscopy and multivariate curve resolution study, J. Phys. Chem. B 117 (2013) 16479–16485, https://doi.org/10.1021/jp4100697.

[2] A.M.P. Neto, O. Sala, The effect of temperature and LiClO4 in the water structure: a raman spectroscopy study, Braz. J. Phys. 34 (2004) 137–141, https://doi.org/10.1590/S0103-97332004000100017.

[3] R. Li, Z. Jiang, Y. Guan, H. Yang, B. Liu, Effects of metal ion on the water structure studied by the Raman O□H stretching spectrum, J. Raman Spectrosc. 40 (2009) 1200–1204, https://doi.org/10.1002/jrs.2262.

[4] C.A. Daly Jr., L.M. Streacker, Y. Sun, S.R. Pattenaude, A.A. Hassanali, P. B. Petersen, S.A. Corcelli, D. Ben-Amotz, Decomposition of the experimental raman and infrared spectra of acidic water into proton, special pair, and counterion contributions, J. Phys. Chem. Lett. 8 (2017) 5246–5252, https://doi.org/10.1021/acs.jpclett.7b02435.

[5] J. Kapitán, M. Dračínský, J. Kaminský, L. Benda, P. Bouř, Theoretical Modeling of Magnesium Ion Imprints in the Raman Scattering of Water, J. Phys. Chem. B 114 (2010) 3574–3582, https://doi.org/10.1021/jp9110508.

[6] P. Jungwirth, D.J. Tobias, Specific Ion Effects at the Air/Water Interface, Chem. Rev. 106 (2006) 1259–1281, https://doi.org/10.1021/cr0403741.

[7] J. Palacký, P. Mojzeš, J. Bok, SVD-based Method for Intensity Normalization, Background Correction and Solvent Subtraction in Raman Spectroscopy Exploiting the Properties of Water Stretching Vibrations, J. Raman Spectr. 42 (2011) 1528–1539, https://doi.org/10.1002/jrs.2896.

[8] Q. Yang, J. Bloino, H. Šestáková, J. Šebestík, J. Kessler, J. Hudecová, J. Kapitán, P. Bouř, Combination of Resonance and Non-Resonance Chiral Raman Scattering in a Cobalt(III) Complex, Angew. Chem. Int. Ed. 62 (2023) e202312521.

[9] G. Zając, P. Bouř, Measurement and Theory of Resonance Raman Optical Activity for Gases, Liquids, and Aggregates. What It Tells about Molecules, J. Phys. Chem. B 126 (2022) 355–367, https://doi.org/10.1021/acs.jpcb.1c08370.

[10] D.A. Case, I.T.E. Cheatham, T. Darden, H. Gohlke, R. Luo, J.K.M. Merz, A. Onufriev, C. Simmerling, B. Wang, R. Woods, The Amber biomolecular simulation programs, J. Comput. Chem. 26 (2005) 1668–1688, https://doi.org/10.1002/jcc.20290.

[11] N. Kamiya, Y.S. Watanabe, S. Ono, J. Higo, AMBER-based hybrid force field for conformational sampling of polypeptides, Chem. Phys. Lett. 401 (2005) 312–317, https://doi.org/10.1016/j.cplett.2004.11.070.

[12] W.L. Jorgensen, J. Chandrasekhar, J.D. Madura, Comparison of simple potential functions for simulating liquid water, J. Chem. Phys. 79 (1983) 926–935, https://doi.org/10.1063/1.445869.

[13] A.D. Becke, Density-functional thermochemistry. III. The role of exact exchange, J. Chem. Phys. 98 (1993) 5648–5652, https://doi.org/10.1063/1.464913.

[14] M. Cossi, V. Barone, Analytical second derivatives of the free energy in solution by polarizable continuum models, J. Chem. Phys. 109 (1998) 6246–6254, https://doi.org/10.1063/1.477265.

[15] P. Bouř, T.A. Keiderling, Partial optimization of molecular geometry in normal coordinates and use as a tool for simulation of vibrational spectra, J. Chem. Phys. 117 (2002) 4126–4132, https://doi.org/10.1063/1.1498468.

[16] P. Michal, J. Kapitán, J. Kessler, P. Bouř, Low-frequency Raman optical activity provides insight into the structure of chiral liquids, Phys. Chem. Chem. Phys. 24 (2022) 19722–19733, https://doi.org/10.1039/D2CP02290G.

[17] P. Bouř, J. Sopková, L. Bednárová, P. Maloň, T.A. Keiderling, Transfer of molecular property tensors in Cartesian coordinates: A new algorithm for simulation of vibrational spectra, J. Comput. Chem. 18 (1997) 646–659, https://doi.org/10.1002/(SICI)1096-987X(19970415)18:5<646::AID-JCC6>3.0.CO;2-N.

[18] S. Yamamoto, X. Li, K. Ruud, P. Bouř, Transferability of various molecular property tensors in vibrational spectroscopy, J. Chem. Theory Comput. 8 (2012) 977–985, https://doi.org/10.1021/ct200714h.

[19] M. Born, K. Huang, Dynamical Theory Of Crystal Lattices, Oxford Academic, Oxforn, 1996.

[20] O. Škrna, J. Kessler, Z. Liu, S. Che, P. Bouř, Reproduction of Chiral Anisotropy in Surface-Enhanced Raman Scattering on Gold Nanowires by Computational Modeling, J. Phys. Chem. C 128 (2024) 12649–12656, https://doi.org/10.1021/acs.jpcc.4c02703.

[21] S. Ding, E. You, Z. Tian, M. Moskovits, Electromagnetic theories of surface-enhanced Raman spectroscopy, Chem. Soc. Rev. 46 (2017) 4042–4076, https://doi.org/10.1039/C7CS00238F.

[22] L.D. Barron, Molecular Light Scattering and Optical Activity, Cambridge University Press, Cambridge, UK, 2004.

[23] P. Bouř, D. Michalík, J. Kapitán, Empirical Solvent Correction for Multiple Amide Group Vibrational Modes, J. Chem. Phys. 122 (2005) 144501, https://doi.org/10.1063/1.1877272.

[24] Q. Wan, L. Spanu, G.A. Galli, F. Gygi, Raman Spectra of Liquid Water from Ab Initio Molecular Dynamics: Vibrational Signatures of Charge Fluctuations in the Hydrogen Bond Network, J. Chem. Theory Comput. 9 (2013) 4124–4130, https://doi.org/10.1021/ct4005307.

[25] T. Morawietz, O. Marsalek, S.R. Pattenaude, L.M. Streacker, D. Ben-Amotz, T. E. Markland, The Interplay of Structure and Dynamics in the Raman Spectrum of Liquid Water over the Full Frequency and Temperature Range, J. Phys. Chem. Lett. 9 (2018) 851–857, https://doi.org/10.1021/acs.jpclett.8b00133.

[26] Q. Yang, J. Kapitán, P. Bouř, J. Bloino, Anharmonic Vibrational Raman Optical Activity of Methyloxirane: Theory and Experiment Pushed to the Limits, J. Phys. Chem. Lett. 13 (2022) 8888–8892, https://doi.org/10.1021/acs.jpclett.2c02320.

[27] V.S.S. Inakollu, H. Yu, A systematic benchmarking of computational vibrational spectroscopy with DFTB3: Normal mode analysis and fast Fourier transform dipole autocorrelation function, J. Comput. Chem. 39 (2018) 2067–2078, https://doi.org/10.1002/jcc.25390.